analytical chemistry

Article

Cite This: *Anal. Chem.* 2019, 91, 3429−3435

pubs.acs.org/ac

Polymerase Chain Reaction-Dynamic Light Scattering Sensor for DNA and Protein by Using Both Replication and Cleavage Properties of Taq Polymerase

Jing Wang, Tingting Li, Ruidi Shen, Gongke Li, and Liansheng Ling*

School of Chemistry, Sun Yat-Sen University, Guangzhou 510275, P. R. China

Supporting Information

ABSTRACT: The incorporation of AuNPs into polymerase chain reaction (PCR) has become a promising strategy to develop sensitive sensing platforms, due to desirable optical properties of AuNPs and the exponential amplification power of PCR. However, the combination of AuNPs to PCR usually fails to reach expected sensitivity along with additional steps. Here we report a one-step and universal PCR-based biosensor for size-dependent detection of nucleic acids and proteins by using the dynamic light scattering (DLS) technique. This sensing system employs a DNA modified AuNPs (AuNPs-DNA) probe to serve as the TaqMan like signal probe, in which DNA on the surface of AuNPs can be cleaved by Taq polymerase during the extension process of PCR, causing the aggregation of AuNPs to be detected by DLS. This strategy enables sequence-specific recognition of target double-stranded DNA (dsDNA), overcoming the background signal change that triggered by the increase of the PCR cycle. It further demonstrates its applicability in detecting a foodborne pathogen *Listeria monocytogenes* with a detection limit of 1.2 fg μL^{-1}, which is more sensitive than colorimetric methods. Moreover, by utilizing a proximity assay strategy, this biosensor shows the capability to the homogeneous detection of protein, showing a detection limit of 1.0 pM for a model thrombin. Together, the work demonstrates a reliable strategy to incorporate AuNPs into PCR amplification process as a signal probe, instead of the post-PCR process.

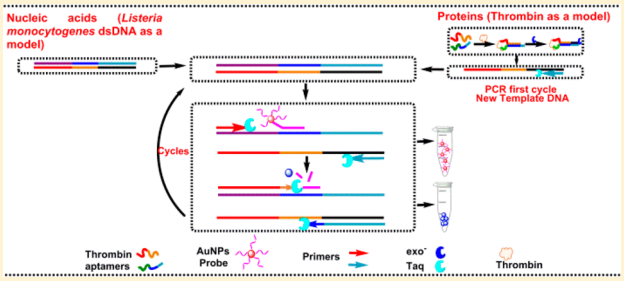

Polymerase chain reaction (PCR) is a powerful nucleic acid amplification-based molecular diagnostic method, which can produce 10^6−10^9 copies of the target.[1] PCR is also capable of amplifying long DNA targets such as kilobase (kb) regions, which is vital to diagnostic applications.[2] Traditionally, PCR products are identified by polyacrylamide gel electrophoresis (PAGE), which has low sensitivity and is time-consuming.[3,4] To overcome these limitations, other alternative methods for detection of PCR products have been developed, such as radioactivity,[5,6] fluorescence,[7,8] electrochemistry,[9,10] surface enhanced resonance Raman scattering (SERRS),[11,12] circular dichroism (CD) spectroscopy,[13] and colorimetric method.[14] Among these methods, real-time fluorescence PCR (RT-PCR) has become a gold standard for many targets due to its sensitivity, repeatability, speed, and ease of operation. However, its background increases dramatically when the cycle number is higher than 35, which might give false positive results and affect its applications.[4,15] Moreover, small-molecule dyes employed are usually limited by their quantum yield and photostability and also interfered with autofluorescence of biological samples.[16−21]

Gold nanoparticles (AuNPs) are extensively explored as a kind of alternative signal reporter in biosensors,[22,23] due to their high photostability, ease of synthesis and easy functionalization with biomolecules including DNA[24,25] and strong light absorption and scattering properties.[26] These desirable properties have resulted in intense development of AuNPs-based colorimetric assays for a range of analytes including metal ions,[27] small molecules,[28] and biomolecules,[22] enabling visual detection in a convenient manner,[29] but these assays suffer from low sensitivity.[30] Recently, dynamic light scattering (DLS) has been introduced into AuNPs-based assay as a detection technique, which is directly used to monitor the size change of AuNPs caused by analytes.[31] DLS is used to be a common optical technique for characterizing size distribution of particles (or macromolecules) in suspension.[32] AuNPs are capable of high light scattering ability, allowing them to be detected by DLS as low as 10^{-16} M, and their light scattering intensity is proportional to particle size.[33] Moreover, the light scattering signal of AuNPs is much higher than interfering substances from most biological samples, which 80 nm AuNPs even show a 10^5 times stronger signal than an organic dye.[34] Therefore, AuNPs have been investigated as DLS probes to develop biosensors for sensitive detection of metal ions,[35,36] DNA,[32,37,38] small molecules,[39] and other biomolecules.[40]

Considering desirable properties of AuNPs and the exponential amplification power of PCR, considerable efforts have been devoted to the combination of AuNPs to PCR.

Received: October 28, 2018
Accepted: February 4, 2019
Published: February 4, 2019

DOI: 10.1021/acs.analchem.8b04929
Anal. Chem. 2019, 91, 3429−3435

Most studies focus on the combination of AuNPs to conventional PCR methods to improve their sensitivity, specificity, or/and efficiency, but these methods require traditional methods including PAGE to identify PCR products.[41−45] AuNP-based biobarcode assays are also developed for the sensitive detection of nucleic acids and proteins,[46−48] which result in single-stranded DNA (ssDNA) generally analyzed by PCR, but these assays involve multistep, tedious separation process. Alternatively, AuNPs are used as signal probes in the post-PCR process to simplify sensing systems. Since ssDNA can bind on the surface of AuNPs to prohibit their aggregation, few assays have been developed based on the effect on the aggregation of AuNPs posed by ssDNA of PCR products for targets.[49−51] Instead of nonspecific recognition of ssDNA to AuNPs, oligonucleotide modified AuNPs are also applied to specifically recognize DNA of PCR products, potentially raising specificity.[14,52] However, these methods usually interfere with byproducts of PCR and involve more than one step.

Inspired by the role of TaqMan in real-time PCR, here we propose to employ DNA modified AuNPs (AuNPs-DNA) as the TaqMan like probe, developing a one-step, homogeneous PCR-based detection method for DNA and proteins. AuNPs-DNA is excised to release AuNPs by utilizing both the replication property and cleave property of Taq polymerase during the PCR process, causing the aggregation of AuNPs. The aggregation of AuNPs results in size changes of AuNPs, which is measured by DLS in a highly sensitive manner. This new PCR-based method shows the capability of one-pot detecting DNA and proteins. It also overcomes the optical interference inherently existing in real-time PCR. To our knowledge, this is the first universal size-dependent PCR-based biosensor for nucleic acids and proteins detection.

EXPERIMENTAL SECTION

PCR Amplification of DNA. The sequences for PCR amplification are shown in Table S1, the total volume of the PCR mixture was 50 μL, it contained 5 μM primer (Oligo 8 and Oligo 9, Table S1), 1 U Taq Polymerase, 200 μM of each dNTP, 2.5 mM $MgCl_2$, 7.4 nM AuNPs-Oligo 1 probe, 1× reaction buffer. For the PCR amplification process, 2 μL of DNA (Oligo 2 and Oligo 3 or *Listeria monocytogenes* DNA) was used. Each set of PCR amplification included a negative control (no template DNA). Amplification of the DNA in the DNA detection was performed using the conditions: 94 °C for 3 min for initial denaturation, cycling (30 cycles) of 94 °C for 20 s, 51 °C for 30 s, 72 °C for 30 s, and 72 °C for 3 min for final extension. The PCR product was detected by DLS and colorimetric technique, respectively.

PCR Amplification of Thrombin. Oligo 10 and Oligo 11 were denatured at 95 °C for 5 min, and gradually cooled to room temperature. A volume of 2 μL of thrombin was mixed with 2 μL of 0.4 nM Oligo 10 and Oligo 11 in reaction solution containing 20 mM Tris-OAc (pH 7.9), 50 mM KOAc, 10 mM $Mg(OAc)_2$, and 1 mM DTT at 37 °C for 30 min. Then, 0.5 U of Klenow fragment (exo^-) polymerase and 1.0 μL of 10 mM dNTPs were added into the 10 μL total mixture volume at 37 °C for 30 min and heated to 95 °C to inactivate the Klenow fragment (exo^-) polymerase. After that, the inactivated mixture acted as a PCR template for the following PCR amplification. The total volume of PCR mixture was 50 μL, it contained 5 μM primer (Oligo 12 and Oligo 13, Table S1), 1 U Taq Polymerase, 200 μM of each dNTP, 2.5 mM $MgCl_2$, 7.4 nM AuNPs-Oligo 1 probe, and 1× reaction buffer. For the PCR amplification process, 2 μL of template DNA (Oligo 10 and Oligo 11) was used. Each set of PCR amplification included a negative control (no thrombin). Amplification of DNA in the thrombin detection was performed using the conditions: 94 °C for 3 min for initial denaturation, cycling (30 cycles) of 94 °C for 20 s, 58 °C for 30 s, 72 °C for 30 s, and 72 °C for 3 min for final extension. The PCR product was detected by DLS and the colorimetric technique, respectively, without further handling.

DLS Measurements. DLS analysis of all AuNPs suspensions was performed on an Elite Sizer nanoparticle/Zeta potentiometer. The measured scattering light intensity was displayed as photon count rate with a unit of kilo count per second ($kc{\cdot}ps^{-1}$). And the operating conditions were: 25 °C of temperature, 90° of detector angle, 683 nm of incident laser wavelength, and 100 mW of laser power. All sizes were based on the intensity average, and each particle size was the average of three measurements.

RESULTS AND DISCUSSION

Principle for the Target Assay. The strategy for detecting double-stranded DNA (dsDNA) was shown in Scheme 1, and

Scheme 1. Schematic Illustration of the Size-Dependent Detection Platform

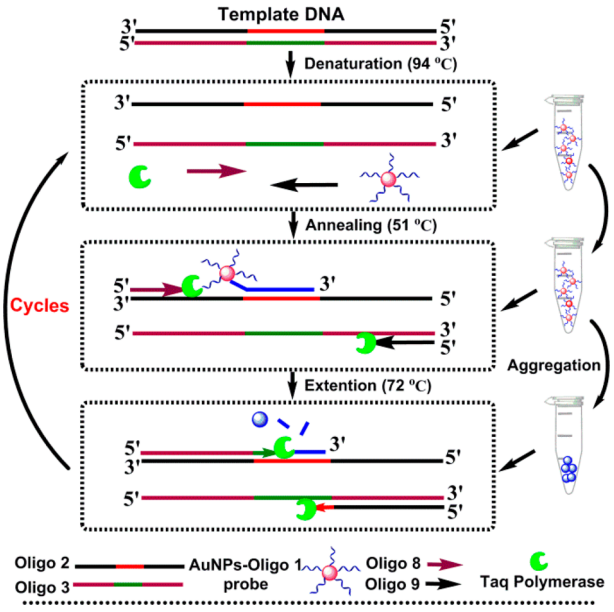

it relies on PCR amplification and the assembly of AuNPs in the salt solution (Scheme 1). The sensing system consists of a template DNA and two primers, Taq polymerase as a mechanical activator in the existence of Mg^{2+}, which Mg^{2+} serves as a cofactor for Taq polymerase, and the AuNPs-DNA as a signal probe. The DNA sequence of AuNPs-DNA probe is complementary to the template dsDNA sequence, which can hybridize to template dsDNA ahead of the primers during an annealing process. In detail, the template dsDNA consisting of Oligo 2 and Oligo 3 is denatured at 94 °C, then it is annealed at 51 °C. AuNPs-Oligo 1 probe, Primer 1 (Oligo 8), and Primer 2 (Oligo 9) hybridize to Oligo 2 and Oligo 3 during the annealing process through the base complementary hybridization,[53] the extension is then carried out at 72 °C. Template

DOI: 10.1021/acs.analchem.8b04929
Anal. Chem. 2019, 91, 3429−3435

DNA is replicated at this stage, accompanied with the cleavage of Oligo 1 on the surface of AuNPs by utilizing both the replication property and cleaving property of Taq polymerase during the PCR process.[54] With the increase of the PCR cycle, the number of Oligo 1 on AuNPs decreases, resulting in the generation of AuNPs with little Oligo 1 modification even bare AuNPs. The resulting AuNPs will aggregate in the high salt buffer which is provided by high Mg^{2+} concentration, while AuNPs-DNA has good stability in the same buffer due to the repulsion of negative charges among the DNA.[55] The aggregation of AuNPs enables size measurement by the DLS technique in a sensitive manner.

Feasibility Study of the Target Assay. To investigate the feasibility of the strategy, a 69 bp dsDNA (Oligo 2 and Oligo 3) was designed and purchased, which is the same as the partial sequence of *Listeria monocytogenes*. This dsDNA was employed as a template dsDNA to be investigated by DLS, transmission electron microscopy (TEM), and UV−vis absorption spectroscopy. As demonstrated in Figure 1A,1B,

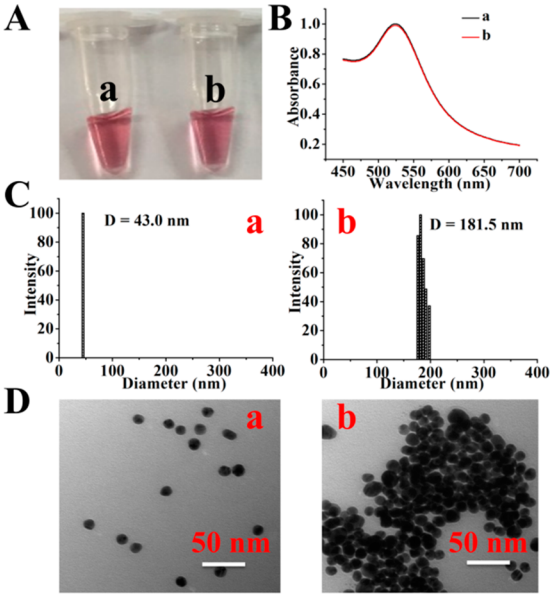

Figure 1. (A) Photograph of the AuNPs solution color. (B) UV−vis absorption spectra of the PCR-DLS sensing method. (C) DLS of the PCR-DLS sensing method. (D) TEM of the PCR-DLS sensing method: (a) PCR product in the absence of template DNA and (b) PCR product in the presence of 1.0 pM template DNA.

there were little color change along with almost no change for the absorption spectra in the absence/presence the addition of 1.0 pM template target DNA, presumably due to the low sensitivity of the colorimetric technique. There was a dramatic change in hydrodynamic diameter before and after the addition of 1.0 pM template target DNA. In the absence of template DNA, the hydrodynamic diameter of the PCR product was 43.0 nm, while it increased to 171.4 nm with the addition of 1.0 pM template dsDNA (Figure 1C). This result indicated that the presence of the template dsDNA can cause the aggregation of AuNPs. TEM images further confirmed this result, which showed that AuNPs were well-dispersed before the addition of 1.0 pM template dsDNA, while they aggregated after the addition of the template (Figure 1D). It is noted that the hydrodynamic diameter from DLS is larger than the size from TEM images. This can be explained by principles of these two techniques, in which DLS is an intensity-based technique, while TEM is a number-based particle size measurement making them fundamentally different.[56,57] Moreover, TEM provides the size information on nanoparticles in the dry state, while DLS gives the hydrodynamic diameter of nanoparticles in the solvated state. The agarose gel electrophoresis for the PCR product was also investigated, and the result showed that there were no bands in the absence of the template, while a band at 69 bp was observed for the template (Figure S3). These results indicate that this assay can detect dsDNA by measuring size changes of AuNPs in the salt solution. These also demonstrate that DLS is more sensitive than the corresponding colorimetric method, indicating DLS might be a sensitive technique for the detection of PCR product.

Optimization of Assay Conditions. This assay was established based on the aggregation of the AuNPs during the PCR process, so the concentration of AuNPs-DNA and PCR cycle number may affect the sensitivity of the assay and both of them were optimized. The diameter difference value (ΔD) between the absence and presence of template DNA was used for the optimization. As shown in Figure S1A, the diameter of AuNPs-Oligo 1 increased with its concentration during the range of 0.37−7.4 nM, reaching a plateau at 7.4 nM in the presence of template dsDNA, which showed a similar tendency with that of the curve for ΔD versus the concentration of AuNPs-Oligo 1, thereby 7.4 nM of AuNPs-Oligo 1 was used in the following experiments. The PCR cycle number was then investigated, and the result shows that maximum ΔD was obtained at the PCR cycle number of 30 (Figure S1B), thereby 30 of the PCR cycle was used throughout this work. In addition, the effect of the sizes of the AuNPs on the assay was also investigated using 5 nm, 13 nm, 20 nm, and 40 nm of AuNPs. The Oligos were modified on the AuNPs of different sizes according to a previous procedure.[58] The results showed that 13 nm AuNPs exhibited the maximum ΔD under the same conditions (Figure S1C), presumably due to that 13 nm AuNPs had the highest DNA attachments under the modification conditions.[59,60] This was further confirmed by TEM images (Figure S2), thereby 13 nm AuNPs were continually used in the following experiments. In addition, the effect of the length of Oligo 1 on the assay was also investigated, and the results showed that 16 bases of Oligo 1 on AuNPs exhibited the best performance (Figure S1D).

Linear Response and Specificity of the Assay to the Template. The linear response to an analyte is the key to an assay, so the response to the different concentrations of the template dsDNA of this assay was investigated by DLS. As shown in Figure 2A, the diameter increased linearly with the logarithm of the dsDNA concentration from 3.0 fM to 1.0 nM, with a linear regression equation of $D = 42.82 + 44.47 \lg C$ (C, fM) and a detection limit of 1.1 fM (3δ/slope). As a comparison, this biosensor was also applied to detect the template dsDNA using the colorimetric technique. The result showed that there was a good linear relationship between the absorbance and the logarithm of the DNA concentration between 1.0 pM and 100 nM, with a detection limit of 0.4 pM (3δ/slope) (Figure S4), which is much higher than that for the DLS technique. These results demonstrate this biosensor's capacity to linearly respond to template dsDNA in a highly sensitive manner, presumably due to the combination of PCR amplification power and the high sensitivity of DLS.

To further explore the effect of nonspecific amplification on this assay, lambda-DNA was employed as a template because

DOI: 10.1021/acs.analchem.8b04929
Anal. Chem. 2019, 91, 3429−3435

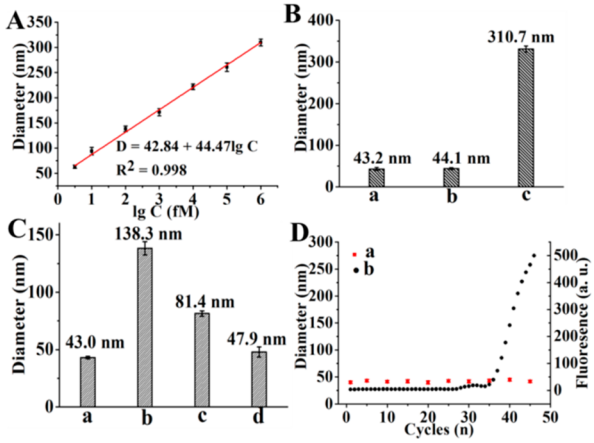

Figure 2. (A) Calibration curve of DLS diameter versus the logarithm of concentration for template DNA ranging from 3.0 fM to 1.0 nM. (B) Effect of nonspecific contamination of PCR amplification (lambda-DNA) on DLS assay: (a) PCR product in the absence of template DNA, (b) PCR product in the presence of 1.0 nM lambda-DNA, and (c) PCR product in the presence of 1.0 nM template DNA (Oligo 2 and Oligo 3). (C) Base mismatched effect on the DLS detection for PCR product: (a) PCR product in the absence of template DNA, (b) PCR product in the presence of 100.0 fM Oligo 2 and Oligo 3 as template DNA, (c) PCR product in the presence of 100.0 fM Oligo 4 and Oligo 5 as template DNA, and (d) PCR product in the presence of 100.0 fM Oligo 6 and Oligo 7 as template DNA. (D) Effect of cycle number on the background signal of PCR-DLS assay and fluorescence PCR method, respectively: (a) PCR-DLS assay in the absence of template DNA and (b) SYRB-Green based fluorescence PCR in the absence of template DNA. The error bars indicate the standard deviations of three replicates.

of its complex duplex structure.[61,62] As shown in Figure 2B, the presence of 1.0 nM lambda-DNA had a negligible effect on the diameter of the system, whereas that for 1.0 nM template DNA dramatically increased to 310.7 nm. These results demonstrate that this assay is free of the interference of nonspecific PCR amplification from contaminated DNA.

Conventional PCR methods usually suffer from the problem of sequence-specific recognition of template dsDNA.[63] To certify the sequence specificity of our method,[64] another two complementary DNA sequences (Oligo 4 and Oligo 5; Oligo 6 and Oligo 7) were designed. The dsDNA formed by Oligo 4 and Oligo 5 has one different base pair from that of the template dsDNA, while the dsDNA formed by Oligo 6 and Oligo 7 has two different base pairs from that of the template. The results showed that the diameter for the template dsDNA was 138.3 nm, while that for dsDNA formed by Oligo 4 and Oligo 5 was 81.4 nm and that for dsDNA formed by Oligo 6 and Oligo 7 was 47.9 nm, which was almost same as the background (43.0 nm) (Figure 2C). In addition, the effect of the location of one mismatched base was also investigated. The result showed that the diameter for the system decreased when the mismatched base was located in the middle of the AuNPs probe recognition site (Figure S5). Together, these results reveal that the proposed assay has the ability of highly sequence-specific recognition.

On the other hand, the background of real-time PCR is always dramatically increased when the cycle number is over 35. To explore the effect of cycle number on the background of our method, the effect of cycle number on the background of our method and real-time PCR were investigated, respectively. As demonstrated in Figure 2D, the background of this assay remained stable even the cycle number increased to 45. In contrast, the background of real-time PCR increased dramatically over the cycle number of 35 (Figure 2D), which was in good accordance with the report.[4] These results indicate that our assay effectively overcomes the effect of nonspecific PCR, reducing background signal. The phenomena might be due to this sensing strategy not only depends on the recognition of template dsDNA with two primers but also depends on the recognition property of the AuNPs-DNA probe, ensuring that nonspecific-PCR amplifications fail to trigger the change of AuNPs diameter.

Application to *Listeria monocytogenes* dsDNA Detection. Encouraged by the results above, this assay was applied to detect *Listeria monocytogenes* by using DLS, which is a fetal human foodborne pathogen with a high case fatality rate.[65] *Listeria monocytogenes* dsDNA was extracted according to a reported method. As the 69 bp dsDNA (Oligo 2 and Oligo 3) was designed to serve as a model for *Listeria monocytogenes*, Oligo 8 and Oligo 9 were still used as primers to recognize *Listeria monocytogenes* dsDNA during the PCR amplification and DLS results showed there was a good linear relationship between the diameter size and the logarithm of the DNA concentration from 8.0 fg μL^{-1} to 0.8 ng μL^{-1}, with a detection limit of 1.2 fg μL^{-1} ($LOD_{lg\,C} = 3\delta/slope$) (Figure 3A). As a

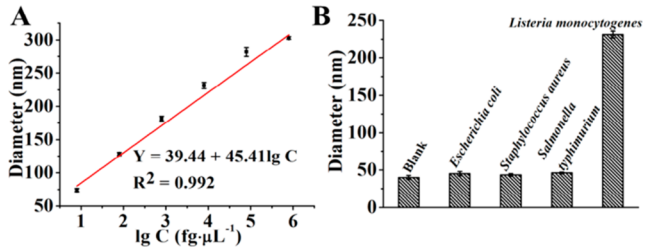

Figure 3. (A) Calibration curve of DLS diameter versus the logarithm of concentration for *Listeria monocytogenes* DNA ranging from 8.0 fg μL^{-1} to 0.8 ng μL^{-1}. (B) DLS selectivity of the proposed method for *Listeria monocytogenes* DNA. The concentration of *Escherichia coli*, *Salmonella typhimurium*, and *Staphylococcus aureus* was 80.0 pg μL^{-1}, respectively, *Listeria monocytogenes* DNA is 8.0 pg μL^{-1}. The error bars indicate the standard deviations of three replicates.

comparison, the sensing performance of this biosensor to *Listeria monocytogenes* was also examined by the colorimetric technique. The results showed that there was a good linear relationship between the absorbance and the logarithm of the DNA concentration between 8.0 pg μL^{-1} and 0.8 μg μL^{-1} (Figure S6), with a detection limit of 1.0 pg μL^{-1} (3δ/slope), which is much higher than that of DLS. These results demonstrate that this biosensor enables highly sensitive detection of *Listeria monocytogenes* by using DLS. To further explore the selectivity of this biosensor for *Listeria monocytogenes* DNA, 10-fold excess *Escherichia coli*, *Salmonella typhimurium*, and *Staphylococcus aureus* DNA were examined compared with 8.0 pg μL^{-1} of *Listeria monocytogenes* dsDNA, respectively. As shown in Figure 3B, there were negligible changes in the presence of other interfering bacteria DNA compared to the background signal. Moreover, the effect of other potential interfering species including metal ions (Cu^{2+}, Ca^{2+}), anions (NO_3^-, SO_4^{2-}), cysteine (Cys), and glutathione (GSH) were also investigated, and only negligible changes were observed (Figure S7). These results indicate that the

DOI: 10.1021/acs.analchem.8b04929
Anal. Chem. 2019, 91, 3429−3435

proposed method has high selectivity for *Listeria monocytogenes*.

To investigate the ability of this biosensor in complicated biological matrixes, the recovery experiment was also conducted in the system containing 2% cell lysis buffer. As shown in Table 1, different concentration of *Listeria monocytogenes* dsDNA was added into each cell lysis buffer and the recovery varied from 98.7% to 103.2%, while the relative standard deviation (RSD) varied from 1.1% to 5.0%. These results indicate that the spiked dsDNA can be accurately detected in these samples by DLS, demonstrating its potential application in the detection of *Listeria monocytogenes* DNA in a biological system.

Table 1. Recoveries of *Listeria monocytogenes* DNA from the Spiked Cell Lysis Buffer

samples	added (fg μL^{-1})	found (fg μL^{-1})	recovery (%)	RSD (%)
Listeria monocytogenes DNA	8.0	7.9	98.7	1.1
	80.0	82.6	103.2	4.0
	800.0	799.6	99.9	5.0

Application to Thrombin Detection. To explore the possibility of applying the proposed method to protein detection, we selected thrombin as a protein model with this sensing system, owing to that thrombin's role in blood hemostasis and clinical diagnosis of the related diseases.[66] For PCR-based protein detection, the information on proteins needs to be converted into the detection of nucleic acids. Proximity assays utilize two or more DNA modified affinity reagents to bind in close proximity to the same protein, giving rise to amplifiable reporter molecules via ligation or polymerization reactions for sensitive proteins detection, protein modifications, or protein−protein interaction studies.[67,68] Thus, we reasoned that ssDNA-based affinity probes containing target protein aptamers may serve as dsDNA template for PCR in our system, enabling sensitive and universal detection of proteins. Two ssDNA-based affinity probes containing thrombin aptamers were previously reported to hybridize to form a template of PCR upon the binding of thrombin,[69] so we designed two thrombin aptamers containing ssDNA (Oligo 10 and Oligo 11) to serve as a template of the assay in the presence of thrombin. The scheme is shown in Scheme 2; thrombin is first recognized by Oligo 10 and Oligo 11, and the partial sequence is extended with the Klenow fragment (exo^-) polymerase to obtain new template dsDNA within the first cycle of PCR. The resulting template is then recognized by Primers 3 and 4 (Oligo 12 and Oligo 13) for PCR amplification, accompanied with the cleavage of Oligo 1 on the surface of AuNPs in the following cycles. The number of Oligo 1 on the AuNPs-DNA probe will decrease with the increase of the PCR cycle, leading to the aggregation of AuNPs in the high salt buffer which is provided by high Mg^{2+} concentration. Therefore, the concentration of thrombin is transformed into the diameter change of AuNPs-DNA probe, which can be estimated by using DLS.

We first examined the feasibility of this assay to detect thrombin by using DLS, the result show the addition thrombin of can obviously increase the diameter of the PCR product (Figure 4A). To further confirm its feasibility, agarose gel electrophoresis for PCR products was investigated. As shown in Figure S8, there were no bands in the absence of thrombin,

Scheme 2. Schematic Illustration of Detection of Thrombin

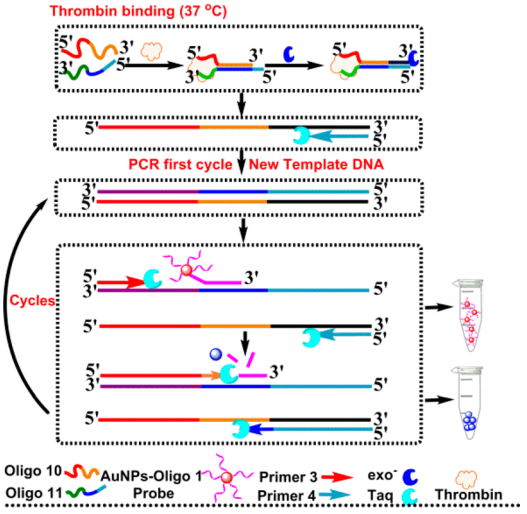

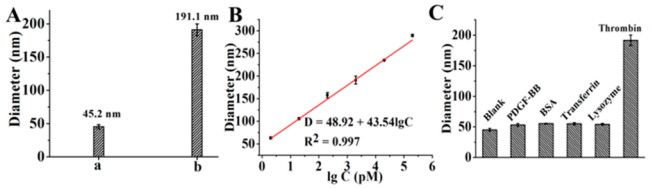

Figure 4. (A) DLS results of the PCR-DLS sensing thrombin: (a) PCR product in the absence of thrombinand (b) PCR product in the presence of 2.0 nM thrombin. (B) Calibration curve of DLS diameter versus the logarithm of concentration for thrombin ranging from 2.0 pM to 200 nM. (C) DLS selectivity of the proposed method for thrombin. The concentration of BSA is 10 nM, lysozyme is 10 nM, the apo-transferrin human is 10 nM, PDGF-BB is 10 nM, thrombin is 2.0 nM, and the mixture contains 2.0 nM thrombin and 10 nM other proteins. The error bars indicate the standard deviations of three replicates.

while a band at 107 bp was observed for the presence of thrombin, demonstrating the capability of this method to detect thrombin. The sensitivity of the sensor for thrombin was further investigated by varying the concentration of thrombin, as shown in Figure 4B, the diameter increased linearly with the logarithm of the thrombin concentration over the range from 2.0 pM to 200 nM, the linear regression equation was D = 48.92 + 43.54 lg C (C, pM; R^2 = 0.997), with a detection limit of 1.0 pM (3δ/slope), more sensitive than the existing methods (Table S3). As a comparison, this biosensor was also applied to detect thrombin using the colorimetric technique. Absorbance results show there was a good linear relationship between the absorbance and the logarithm of DNA concentration from 1.0 nM to 20 μM (Figure S9), with a detection limit of 0.57 nM (3δ/slope), which was much higher than that of DLS. These results demonstrate that this biosensor enables highly sensitive detection of thrombin by DLS. To further explore the selectivity of this biosensor for thrombin, 5-fold excess bovine serum albumin (BSA), lysozyme, transferrin human, and platelet-derived growth factor (PDGF)-BB were used as interfering protein to replace 2.0 nM of thrombin, respectively. As shown in Figure 4C, there were negligible changes in the presence of each interfering protein compared to the background signal. Additionally, the effect of other potential interfering species including metal ions (Cu^{2+}, Ca^{2+}), anions (NO_3^-, SO_4^{2-}), Cys, and GSH were also

DOI: 10.1021/acs.analchem.8b04929
Anal. Chem. 2019, 91, 3429−3435

investigated, and only negligible changes were observed (Figure S10). These results indicate that the proposed method has high selectivity for thrombin.

To investigate the ability of this biosensor in complicated biological matrixes, the recovery experiment was also conducted in the system containing 2% human serum. As shown in Table 2, different concentrations of thrombin were added into each human sera solution, the recovery varied from 94.6% to 97.7%, and the RSD varied from 2.8% to 5.3%. These results indicate that the spiked thrombin can be accurately detected in these samples by DLS, demonstrating its potential application in detection of protein in a biological system.

Table 2. Recoveries of Thrombin from the Spiked Human Serum Samples

samples	added (pM)	found (pM)	recovery (%)	RSD (%)
thrombin	2.0	1.89	94.6	5.3
	20.0	19.04	95.2	4.4
	200.0	195.40	97.7	2.8

CONCLUSION

In conclusion, we have successfully developed a one pot, universal PCR-based biosensor for DNA and proteins with the DLS technique. This sensing system uses AuNPs-DNA as a TaqMan like signal probe to recognize the template DNA, which can be then cleaved by Taq polymerase during the extension process after the first PCR cycle, resulting in the aggregation of the AuNPs in the high concentration of Mg^{2+}. Employing a designed dsDNA as a template, this assay shows a linear response behavior in a highly sensitive manner, which is more sensitive than the corresponding colorimetric method. Importantly, as this biosensor depends on the recognition of two primers and the recognition of AuNPs-DNA probe to template dsDNA, it enables sequence-specific recognition of target DNA, showing a PCR cycle number-independent background. This biosensor further demonstrates its applicability by the sensitive and selective detection of *Listeria monocytogenes* and thrombin, even in the spiked samples. Taken together, this biosensor has the capacity of detecting both nucleic acids and proteins, demonstrating the great potential in the development of a universal biosensor for various biomolecule biomarkers.

ASSOCIATED CONTENT

Supporting Information

The Supporting Information is available free of charge on the ACS Publications website at DOI: 10.1021/acs.analchem.8b04929.

Chemicals and reagents, apparatus, partial experimental procedures, and additional characterization data (PDF)

AUTHOR INFORMATION

Corresponding Author

*E-mail: cesllsh@mail.sysu.edu.cn.

ORCID

Jing Wang: 0000-0001-7104-6661

Gongke Li: 0000-0003-3750-6358

Liansheng Ling: 0000-0002-0471-7987

Author Contributions

The manuscript was written through the contributions of all authors. All authors have given approval to the final version of the manuscript.

Notes

The authors declare no competing financial interest.

ACKNOWLEDGMENTS

This work was supported by the National Natural Science Foundation of China (Grants 21375153, 21475153, and 21675178).

REFERENCES

(1) Mullis, K. B.; Faloona, F. A. *Methods Enzymol.* **1987**, *155*, 335−350.

(2) Zhao, Y.; Chen, F.; Li, Q.; Wang, L.; Fan, C. *Chem. Rev.* **2015**, *115*, 12491−12545.

(3) Muyzer, G.; de Waal, E. C.; Uitterlinden, A. G. *Appl. Environ. Microbiol.* **1993**, *59*, 695−700.

(4) Keohavong, P.; Thilly, W. G. *Proc. Natl. Acad. Sci. U. S. A.* **1989**, *86*, 9253−9257.

(5) Nick, H.; Gilbert, W. *Nature* **1985**, *313*, 795−798.

(6) Zitz, J. C.; McLachlin, C. M.; Tate, J. E.; Mutter, G. L.; Crum, C. P. *Mod. Pathol.* **1994**, *7*, 407−411.

(7) Higuchi, R.; Fockler, C.; Dollinger, G.; Watson, R. *Nat. Biotechnol.* **1993**, *11*, 1026−1030.

(8) Sassolas, A.; Leca-Bouvier, B. D.; Blum, L. J. *Chem. Rev.* **2008**, *108*, 109−139.

(9) Hocek, M.; Fojta, M. *Chem. Soc. Rev.* **2011**, *40*, 5802−5814.

(10) Campos-Ferreira, D. S.; Souza, E. V. M.; Nascimento, G. A.; Zanforlin, D. M. L.; Arruda, M. S.; Beltrão, M. F. S.; Melo, A. L.; Bruneska, D.; Lima-Filho, J. L. *Arabian J. Chem.* **2016**, *9*, 443−450.

(11) Graham, D.; Faulds, K. *Chem. Soc. Rev.* **2008**, *37*, 1042−1051.

(12) Xu, L.; Yan, W.; Ma, W.; Kuang, H.; Wu, X.; Liu, L.; Zhao, Y.; Wang, L.; Xu, C. *Adv. Mater.* **2015**, *27*, 1706−1711.

(13) Ma, W.; Kuang, H.; Xu, L.; Ding, L.; Xu, C.; Wang, L.; Kotov, N. A. *Nat. Commun.* **2013**, *4*, 2689.

(14) Deng, H.; Xu, Y.; Liu, Y.; Che, Z.; Guo, H.; Shan, S.; Sun, Y.; Liu, X.; Huang, K.; Ma, X.; Wu, Y.; Liang, X.-J. *Anal. Chem.* **2012**, *84*, 1253−1258.

(15) Diaz, R. S.; Sabino, E. C. *Braz. J. Med. Biol. Res.* **1998**, *31*, 1239−1242.

(16) Wang, W.; Vellaisamy, K.; Li, G.; Wu, C.; Ko, C.-N.; Leung, C.-H.; Ma, D.-L. *Anal. Chem.* **2017**, *89*, 11679−11684.

(17) Aslan, K.; Gryczynski, I.; Malicka, J.; Matveeva, E.; Lakowicz, J. R.; Geddes, C. D. *Curr. Opin. Biotechnol.* **2005**, *16*, 55−62.

(18) Ma, D.-L.; Xu, T.; Chan, D. S. H.; Man, B. Y. W.; Fong, W.-F.; Leung, C.-H. *Nucleic Acids Res.* **2011**, *39*, No. e67.

(19) Wang, W.; Mao, Z.; Wang, M.; Liu, L.-J.; Kwong, D. W.; Leung, C.-H.; Ma, D.-L. *Chem. Commun.* **2016**, *52*, 3611−3614.

(20) He, H.-Z.; Chan, W.-I.; Mak, T.-Y.; Liu, L.-J.; Wang, M.; Chan, D. S.-H.; Ma, D.-L.; Leung, C.-H. *Methods* **2013**, *64*, 218−223.

(21) He, H.-Z.; Wang, M.; Chan, D. S.-H.; Leung, C.-H.; Lin, X.; Lin, J.-M.; Ma, D.-L. *Methods* **2013**, *64*, 212−217.

(22) Saha, K.; Agasti, S. S.; Kim, C.; Li, X.; Rotello, V. M. *Chem. Rev.* **2012**, *112*, 2739−2779.

(23) Wu, X.; Xu, L.; Ma, W.; Liu, L.; Kuang, H.; Kotov, N. A.; Xu, C. *Adv. Mater.* **2016**, *28*, 5907−5915.

(24) Sun, M.; Qu, A.; Hao, C.; Wu, X.; Xu, L.; Xu, C.; Kuang, H. *Adv. Mater.* **2018**, *30*, 1804241.

(25) Shah, P.; Choi, S. W.; Kim, H.-j.; Cho, S. K.; Bhang, Y.-J.; Ryu, M. Y.; Thulstrup, P. W.; Bjerrum, M. J.; Yang, S. W. *Nucleic Acids Res.* **2016**, *44*, No. e57.

(26) Sun, J.; Xianyu, Y.; Jiang, X. *Chem. Soc. Rev.* **2014**, *43*, 6239−6253.

(27) Sener, G.; Uzun, L.; Denizli, A. *ACS Appl. Mater. Interfaces* **2014**, *6*, 18395−18400.

DOI: 10.1021/acs.analchem.8b04929
Anal. Chem. 2019, 91, 3429−3435

(28) Gu, Q.; Nanney, W.; Cao, H. H.; Wang, H.; Ye, T. *J. Am. Chem. Soc.* **2018**, *140*, 14134−14143.
(29) Sun, M.; Xu, L.; Qu, A.; Zhao, P.; Hao, T.; Ma, W.; Hao, C.; Wen, X.; Colombari, F. M.; de Moura, A. F.; Kotov, N. A.; Xu, C.; Kuang, H. *Nat. Chem.* **2018**, *10*, 821−830.
(30) Vial, S.; Berrahal, Y.; Prado, M.; Wenger, J. r. m. *ACS Sens* **2017**, *2*, 251−256.
(31) Jans, H.; Huo, Q. *Chem. Soc. Rev.* **2012**, *41*, 2849−2866.
(32) Miao, X.-M.; Xiong, C.; Wang, W.-W.; Ling, L.-S.; Shuai, X.-T. *Chem. - Eur. J.* **2011**, *17*, 11230−11236.
(33) Yguerabide, J.; Yguerabide, E. E. *Anal. Biochem.* **1998**, *262*, 137−156.
(34) Li, C.; Ma, J.; Fan, Q.; Tao, Y.; Li, G. *Chem. Commun.* **2016**, *52*, 7850−7853.
(35) Kalluri, J. R.; Arbneshi, T.; Khan, S. A.; Neely, A.; Candice, P.; Varisli, B.; Washington, M.; McAfee, S.; Robinson, B.; Banerjee, S.; Singh, A. K.; Senapati, D.; Ray, P. C. *Angew. Chem. Int. Ed.* **2009**, *48*, 9668−9671.
(36) Miao, X.; Ling, L.; Shuai, X. *Chem. Commun.* **2011**, *47*, 4192−4194.
(37) Liu, X.; Dai, Q.; Austin, L.; Coutts, J.; Knowles, G.; Zou, J.; Chen, H.; Huo, Q. *J. Am. Chem. Soc.* **2008**, *130*, 2780−2782.
(38) Yin, H.; Huang, X.; Ma, W.; Xu, L.; Zhu, S.; Kuang, H.; Xu, C. *Biosens. Bioelectron.* **2014**, *52*, 8−12.
(39) Miao, X.; Ling, L.; Shuai, X. *Biosens. Bioelectron.* **2013**, *41*, 880−883.
(40) Miao, X.; Zou, S.; Zhang, H.; Ling, L. *Sens. Actuators, B* **2014**, *191*, 396−400.
(41) Li, H.; Huang, J.; Lv, J.; An, H.; Zhang, X.; Zhang, Z.; Fan, C.; Hu, J. *Angew. Chem. Int. Ed.* **2005**, *117*, 5230−5233.
(42) Li, M.; Lin, Y.-C.; Wu, C.-C.; Liu, H.-S. *Nucleic Acids Res.* **2005**, *33*, e184−e184.
(43) Vu, B. V.; Litvinov, D.; Willson, R. C. *Anal. Chem.* **2008**, *80*, 5462−5467.
(44) Xiao, Y.; Dane, K. Y.; Uzawa, T.; Csordas, A.; Qian, J.; Soh, H. T.; Daugherty, P. S.; Lagally, E. T.; Heeger, A. J.; Plaxco, K. W. *J. Am. Chem. Soc.* **2010**, *132*, 15299−15307.
(45) Lou, X.; Zhang, Y. *ACS Appl. Mater. Interfaces* **2013**, *5*, 6276−6284.
(46) Nam, J.-M.; Thaxton, C. S.; Mirkin, C. A. *Science* **2003**, *301*, 1884−1886.
(47) Nam, J.-M.; Park, S.-J.; Mirkin, C. A. *J. Am. Chem. Soc.* **2002**, *124*, 3820−3821.
(48) Hill, H. D.; Mirkin, C. A. *Nat. Protoc.* **2006**, *1*, 324−336.
(49) Li, H.; Rothberg, L. J. *J. Am. Chem. Soc.* **2004**, *126*, 10958−10961.
(50) Deng, H.; Zhang, X.; Kumar, A.; Zou, G.; Zhang, X.; Liang, X.-J. *Chem. Commun.* **2013**, *49*, 51−53.
(51) Li, F.; Li, F.; Yang, G.; Aguilar, Z. P.; Lai, W.; Xu, H. *Sens. Actuators, B* **2018**, *255*, 1455−1461.
(52) Zou, L.; Shen, R.; Ling, L.; Li, G. *Anal. Chim. Acta* **2018**, *1038*, 105−111.
(53) Hu, P.; Li, M.; Wei, X.; Yang, B.; Li, Y.; Li, C.-Y.; Du, J. *Anal. Chem.* **2018**, *90*, 9751−9760.
(54) Koukhareva, I.; Lebedev, A. *Anal. Chem.* **2009**, *81*, 4955−4962.
(55) Luo, C.; Wen, W.; Lin, F.; Zhang, X.; Gu, H.; Wang, S. *RSC Adv.* **2015**, *5*, 10994−10999.
(56) Bhattacharjee, S. *J. Controlled Release* **2016**, *235*, 337−351.
(57) Zheng, T.; Bott, S.; Huo, Q. *ACS Appl. Mater. Interfaces* **2016**, *8*, 21585−21594.
(58) Elghanian, R.; Storhoff, J. J.; Mucic, R. C.; Letsinger, R. L.; Mirkin, C. A. *Science* **1997**, *277*, 1078−1081.
(59) Liu, B.; Liu, J. *Anal. Methods* **2017**, *9*, 2633−2643.
(60) Zhang, X.; Gouriye, T.; Göeken, K.; Servos, M. R.; Gill, R.; Liu, J. *J. Phys. Chem. C* **2013**, *117*, 15677−15684.
(61) Kurita, R.; Yanagisawa, H.; Yoshioka, K.; Niwa, O. *Biosens. Bioelectron.* **2015**, *70*, 366−371.
(62) Plesa, C.; Ruitenberg, J. W.; Witteveen, M. J.; Dekker, C. *Nano Lett.* **2015**, *15*, 3153−3158.
(63) Wolffs, P.; Knutsson, R.; Sjöback, R.; Rådström, P. *BioTechniques* **2001**, *31*, 766−771.
(64) Vial, S.; Berrahal, Y.; Prado, M.; Wenger, J. *ACS Sens.* **2017**, *2*, 251−256.
(65) Moura, A.; Criscuolo, A.; Pouseele, H.; Maury, M. M.; Leclercq, A.; Tarr, C.; Björkman, J. T.; Dallman, T.; Reimer, A.; Enouf, V. *Nat. Microbiol.* **2017**, *2*, 16185.
(66) Shen, G.; Zhang, H.; Yang, C.; Yang, Q.; Tang, Y. *Anal. Chem.* **2017**, *89*, 548−551.
(67) Blokzijl, A.; Nong, R.; Darmanis, S.; Hertz, E.; Landegren, U.; Kamali-Moghaddam, M. *Biochim. Biophys. Acta, Proteins Proteomics* **2014**, *1844*, 933−939.
(68) Greenwood, C.; Ruff, D.; Kirvell, S.; Johnson, G.; Dhillon, H. S.; Bustin, S. A. *Biomol. Detect. Quantif.* **2015**, *4*, 10−16.
(69) Ma, C.; Cao, L.; Shi, C.; Ye, N. *Chem. Commun.* **2011**, *47*, 11303−11305.

DOI: 10.1021/acs.analchem.8b04929
Anal. Chem. 2019, 91, 3429−3435